populated) — potentially leading to the possibility of inventing terahertz amplifiers and generators relying on transitions between spin subbands (a possibility announced earlier in Ref. [14]).

Figure 5 shows the dependence of the magnetic energy on angle χ for the case of $Z_3 \gg Z_1 \gg Z_2$ and for various values of reverse current density. In this event, the parallel configuration $\chi = 0$ at the threshold current density $j = j_{\text{th}}$ (the same as for the forward current) becomes unstable, switching the system to the stable antiparallel magnetic configuration $\chi = \pi$, which is also stable for forward current (see Fig. 1), so that the switching is irreversible. This behavior can be used to magnetically record one-time (archival) information using spin-polarized current. With the sd-exchange interaction with a characteristic length of $\sim 10^{-6}$ cm underlying the process, extremely high recording density can be achieved.

References

1. Katine J A et al. *Phys. Rev. Lett.* **84** 3149 (2000)
2. Chen T Y, Ji Y, Chien C L *Appl. Phys. Lett.* **84** 380 (2004)
3. Slonczewski J C *J. Magn. Magn. Mater.* **159** L1 (1996)
4. Berger L *Phys. Rev. B* **54** 9353 (1996)
5. Heide C, Zilberman P E, Elliott R J *Phys. Rev. B* **63** 064424 (2001)
6. Gulyaev Yu V, Zil'berman P E, Épshtein É M, Elliott R J *Pis'ma Zh. Eksp. Teor. Fiz.* **76** 189 (2002) [*JETP Lett.* **76** 155 (2002)]
7. Gulyaev Yu V, Zil'berman P E, Epshtein E M, Elliott R J *Zh. Eksp. Teor. Fiz.* **127** 1138 (2005) [*JETP* **100** 1005 (2005)]
8. Elliott R J, Epshtein E M, Gulyaev Yu V, Zilberman P E *J. Magn. Magn. Mater.* **300** 122 (2006)
9. Epshtein E M, Gulyaev Yu V, Zilberman P E, cond-mat/0606102
10. Gulyaev Yu V et al. *Pis'ma Zh. Eksp. Teor. Fiz.* **85** 192 (2007) [*JETP Lett.* **85** 160 (2007)]
11. Gulyaev Yu V, Zil'berman P E, Panas A I, Épshteĭn É M *Pis'ma Zh. Eksp. Teor. Fiz.* **86** 381 (2007) [*JETP Lett.* **86** 328 (2007)]
12. Gulyaev Yu V, Zilberman P E, Krikunov A I, Épshtein É M *Zh. Tekh. Fiz.* **77** (9) 67 (2007) [*Tech. Phys.* **52** 1169 (2007)]
13. Epshtein E M, Gulyaev Yu V, Zilberman P E *J. Magn. Magn. Mater.* **312** 200 (2007)
14. Kadigrobov A K et al. *Europhys. Lett.* **67** 948 (2004)

PACS numbers: **72.25.–b**, **75.75.+a**, **85.75.–d**
DOI: 10.1070/PU2008v051n04ABEH006508
DOI: 10.3367/UFNr.0178.200804i.0436

The generalized Landau – Lifshitz equation and spin transfer processes in magnetic nanostructures

A K Zvezdin, K A Zvezdin, A V Khvalkovskiy

1. Introduction

Recently, a new method for magnetic-body magnetization reversal has been proposed [1, 2] and experimentally substantiated [3–5], based on the fact that a current traversing a magnetic system transfers not only charge but also spin, and constitutes therefore a flux of the angular momentum. Spin polarization of the current (i.e., nonvanishing total spin momentum) arises due to the exchange interaction, for the current flowing through a ferromagnetic. If the current flows from a ferromagnetic to a nonmagnetic material, it retains its polarization over a certain length. However, if the polarized current traverses a nonuniformly magnetized magnetic system, its spin moment has to adjust itself to the system's magnetization. Because spin is locally conserved, the change in the angular momentum of the current is transferred to the ferromagnetic; thus, the divergence in the spin flow gives rise to a torque that acts on the magnetization. Such a process has come to be known as spin transfer. Under certain conditions, the spin transfer can result in the magnetization reversal of magnetic structures, as well as causing spin wave generation and domain wall motion. This effect is quantum in nature and undoubtedly one of fundamental interest.

Adding to the interest in exciting magnetization in this way are the successes achieved and problems encountered in developing MRAM (Magnetoresistance Random Access Memory) elements, microwave devices, and magnetic logic elements [6]. Various aspects of the effect under study were discussed in reviews [6–8].

The theoretical description of spin transfer process in nonuniform ferromagnetic media usually relies on the so-called sd-model which assumes that charge and spin currents are carried by external electrons whose (Bloch) wave functions are primarily formed by the s- and p-orbitals of the material's atoms, while the magnetization is determined by the inner underpopulated d-orbitals (for details see Ref. [9]). In this approach, the sp–d hybridization is assumed to be sufficiently small and responsible for the exchange interaction (with the energy on the order of several tenths of an electron-volt) between the sp and d electrons. The corresponding exchange fields are on the order of or higher than 10^7 Oe.

The mechanism by which the current's spin moment (or more precisely, its *transverse* component [1, 2]) adjusts itself to the direction of the local magnetization is the exchange interaction mentioned above, and because of the large value of the exchange field this adaptation process occurs over distances on the order of 1 nm. This distance is much smaller than the characteristic length of spin–lattice relaxation, which is several dozen nanometers in ferromagnetic metals. Thus, the spin flow is not scattered by the impurities, it is only redistributed. The spin flux $\hat{Q}$ is transferred from moving to localized electrons in the form of torque $\mathbf{T}$ which causes their spins to reorient themselves or to precess; $\hat{Q}$ and $\mathbf{T}$ are defined as $Q_{ij} = \sum v_j S_i$, $T_i = -\nabla_j Q_{ij}$, where $\mathbf{v}$ and $\mathbf{S}$ are, respectively, the velocity and spin vectors, the summation runs over all the electrons of the flow, and i, j are the Cartesian indices. The spin-current-induced dynamics of a nonuniformly magnetized s–d system are described approximately by the generalized Landau–Lifshitz equation (GLLE) involving an additional spin torque $\mathbf{T}_{\text{s.t.}} \equiv \gamma \mathbf{T}$ (where γ is the gyromagnetic ratio):

$$\frac{\mathrm{d}\mathbf{M}}{\mathrm{d}t} = -\gamma \mathbf{M} \times \mathbf{H}_{\text{eff}} + \mathbf{T}_{\text{s.t.}} + \frac{\alpha}{M_{\text{s}}} \left(\mathbf{M} \times \frac{\mathrm{d}\mathbf{M}}{\mathrm{d}t} \right), \qquad (1)$$

where $\mathbf{M}$ is the magnetization vector, t is the time, α is the Gilbert damping parameter, M_{s} is the saturation magnetization, and the effective field $\mathbf{H}_{\text{eff}}$ [10] sums the contributions from the external magnetic field and the magnetostatic, exchange interaction, and anisotropy fields.

Usually, two configurations of planar structure are employed to consider spin transfer processes. In the first and most widely used CPP (current perpendicular to the plane) configuration, the current flows perpendicular to layers in a structure containing layers with different magnetization directions. In the second, CIP (current in the plane) configuration, the current flows along the magnetic layer containing a domain wall (DW).

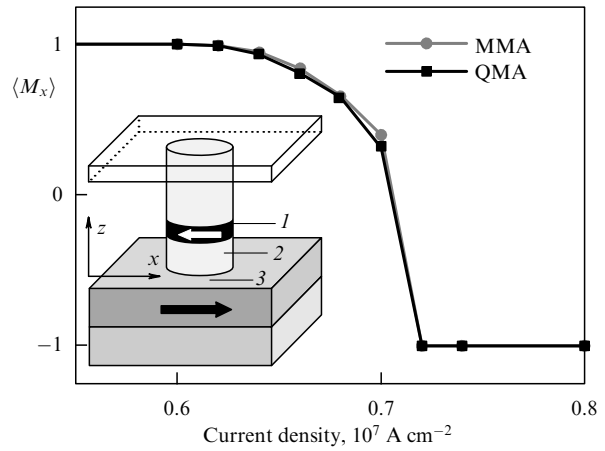

Figure 1. Layer and time averaged and M_s-normalized x-component of magnetization for the free layer of the CPP structure shown in inset, as a function of current through the system (MMA and QMA calculations). Calculation parameters are given in the text. Shown in the inset is a CPP geometry typically used to study the polarized-current-induced magnetization dynamics: *1*, free layer; *2*, intermediate nonmagnetic layer, and *3*, fixed magnetization layer.

The CPP system with a spin transfer (see inset to Fig. 1) is a nanopillar containing a multilayer magnetic structure $N_1/F_1/N/F_2/N_2$ (F and N referring, respectively, to ferromagnetic and nonmagnetic layers) and having an oval-shaped cross section with a typical dimension of 100 nm (the lateral dimensions of the system are determined by the desire to reduce the parasitic influence of the eddy magnetic field from the current flowing through the system). Comprising the nanopillar are (see Fig. 1) a free layer *1* with a thickness of 1–2 nm; a reference layer *3* with a fixed direction of magnetization $\mathbf{m}_{\rm ref}$ (for example, along the x-axis), and a nonmagnetic layer *2* with a thickness on the order of 10 nm (enough to reduce the interlayer exchange interaction to an acceptably small value), which is sandwiched between two above layers. The free-layer magnetic anisotropy, generally determined by the layer's shape, is assumed to be sufficiently small that spin direction in the layer can be easily controlled by an external field and/or a torque.

Spin moment transfer in this system occurs as follows. If we suppose that the magnetic moments in layers *1* and *3* are not collinear and that the electron flux emerges from layer *3*, then the spin flux is defined by a single component $Q_{xz} = -(\hbar/2e)PJ$, where J is the electric current density, and P is the spin polarization of the current (interpreted as the difference-to-sum ratio of partial currents with a spin projection of $1/2$ onto the quantization axis). The partial reflection of polarized carriers at the interfaces between the layers results in the spin flux acquiring a component perpendicular to the magnetizations of both the free and reference layers. The electrons entering layer *1* have their spins rotated by the exchange field to align with the layer's localized spins [11]. We have already mentioned that this process occurs over a length on the order of 1 nm from the interface between layers *1* and *2*, and that in this region div $\hat{Q}$ and the vector $-\mathbf{T}$ equal to it are different from zero. Thus, spin transfer constitutes in fact a surface effect. However, if the free layer is sufficiently thin, then due to exchange rigidity the torque extends its action over the whole of the layer.

The magnetization dynamics of the free layer can be described by the generalized Landau–Lifshitz equation (1). Although the spin torque $\mathbf{T}_{\rm s.t.}$ can be calculated quantum-mechanically [8], for our purposes it suffices to employ a phenomenological approach of the type Landau and Lifshitz used when deriving their equation in 1935 [12].

Let us resolve the vector $\mathbf{T}_{\rm s.t.}$ along three mutually perpendicular axes parallel to the vectors $\mathbf{M}$, $[\mathbf{M}\times\mathbf{m}_{\rm ref}]$, and $\mathbf{M}\times[\mathbf{M}\times\mathbf{m}_{\rm ref}]$, where $\mathbf{m}_{\rm ref}$ is a unit vector directed along the reference layer magnetization. The projection of $\mathbf{T}_{\rm s.t.}$ onto $\mathbf{M}$ is zero because the Landau–Lifshitz equation presupposes the validity of the condition $M = \text{const}$. Two other components of $\mathbf{T}_{\rm s.t.}$, the parallel ($\mathbf{T}_\parallel$) and the perpendicular ($\mathbf{T}_\perp$) to the plane of $(\mathbf{M}, \mathbf{m}_{\rm ref})$, are usually written in the form

$$\mathbf{T}_\parallel = -\frac{\gamma a_J}{M_{\rm s}}\,\mathbf{M}\times[\mathbf{M}\times\mathbf{m}_{\rm ref}]\,, \tag{2}$$

$$\mathbf{T}_\perp = \gamma b_J[\mathbf{M}\times\mathbf{m}_{\rm ref}]\,. \tag{3}$$

Here, the coefficients a_J and b_J (with the dimensionality of the field) are proportional to the current density J and depend on the material parameters and interface characteristics involved. In the general case, a_J and b_J also depend on the angle between $\mathbf{M}$ and $\mathbf{m}_{\rm ref}$ — a dependence which can, however, be neglected in the first approximation [13, 14]. The inequality $|b_J| \ll |a_J|$ holds true for real systems. Typical values of the parameters are as follows: $a_J = 10-100$ Oe for $J = 10^7$ A cm^{-2}; $|b_J/a_J| \sim 0.1$, with a_J and b_J being opposite in sign [15].

There are two regimes in which the magnetic layer of such a structure can be excited by a spin-polarized current. The first occurs when the momentum of the current flowing through such a structure acts — via the spin transfer effect — to reverse the magnetization of the free layer in the direction of one of the stable magnetic states (precisely which depends on the direction of the current) [5]. The second regime is usually achieved by applying a strong (several kOe) magnetic field to the system. In this case, the field and current combined cause the magnetic moment of the free layer to perform high-amplitude oscillations (rotation in the plane of a film being an example) [16]. The polarized current should have a density on the order of 10^7 A cm^{-2} to be able to excite the magnetic structure.

A typical example of a CIP spin transfer system is a thin magnetic film or a nanowire comprising a DW. As current carriers pass through the DW, their spin moment tends at every point of the line of flow to realign with the local magnetization, resulting in the system's magnetization being affected by the torque $\mathbf{T}_{\rm s.t.}$.

Let us write out the components of $\mathbf{T}_{\rm s.t.}$ by analogy with those for CPP systems. In CIP systems, the role of $\mathbf{m}_{\rm ref}$ is played by the vector $(\mathbf{j}_{\rm e}\nabla)\mathbf{M}$ (with $\mathbf{j}_{\rm e}$ being a unit vector along the current) which determines the variation in the magnetization along the lines of current flow. The nonzero Cartesian components of $\mathbf{T}_{\rm s.t.}$ along $\mathbf{M}$, $[\mathbf{M}\times(\mathbf{j}_{\rm e}\nabla)\mathbf{M}]$, $\mathbf{M}\times[\mathbf{M}\times(\mathbf{j}_{\rm e}\nabla)\mathbf{M}]$ vectors are written in the form [17–19]

$$\mathbf{T}_{\rm a} = -\frac{c_J}{M_{\rm s}^2}\,\mathbf{M}\times\left[\mathbf{M}\times(\mathbf{j}_{\rm e}\nabla)\mathbf{M}\right], \tag{4}$$

$$\mathbf{T}_{\rm na} = -\frac{d_J}{M_{\rm s}}\left[\mathbf{M}\times(\mathbf{j}_{\rm e}\nabla)\mathbf{M}\right]. \tag{5}$$

Here, the parameters c_J and d_J are proportional to the current. The components $T_{\rm a}$ and $T_{\rm na}$ are called adiabatic and nonadiabatic torques, respectively. As shown in Refs [17–19], the former describes the effect of spin transfer based on the assumption that the spin subsystem of the

carriers during their passing is at every point of the domain wall in equilibrium with the magnetic system. The second component accounts for how the average spin moment of the electrons deviates from a local magnetization direction. The ratio $\xi_{\mathrm{CIP}} = d_J/c_J$, or the nonadiabaticity of the process, is a material parameter and usually ranges between 0.001 and 0.05 [19]. Experiments on the use of a polarized current to induce domain wall motion are normally carried out on thin films (a few nanometers thick) with a critical current density of about 10^8 A cm^{-2} sufficient for a DW to detach itself from pinning centers [20].

Some significant aspects of the solution of the GLLE (1) for various types of systems are discussed in what follows.

2. On the role of the micromagnetic approach in modeling current-induced magnetization dynamics in CPP structures

Because the width of the domain wall ($\sim 30-50$ nm) in nanopillar CPP structures described in the Introduction is of the same order as the size of the free layer, it is often assumed that the free layer mostly resides in the single-domain state — leading to the belief that the dynamics of the system are adequately described by the macrospin approximation (in which layer magnetization is represented by a unit magnetic moment). Calculations using this approximation do indeed agree qualitatively — and in some cases quantitatively — with the experimental results. However, recent direct observations of polarized-current-induced switching [21] and oscillations [22] show strongly nonuniform magnetization distributions to be involved in their dynamics — a finding which full-scale micromagnetic modeling calculations also support [23, 24]. This raises the question of how far the macrospin approximation can be applied to these processes. Another important point to understand is through the behavior of what parameters and in which way can the difference between the macrospin description of the system and the more realistic micromagnetic description be seen.

To investigate these queries, we simulated the current-induced magnetization dynamics of a nanopillar CPP structure (see the inset to Fig. 1) using both the micromagnetic approximation (MMA) and the quasimacrospin approximation (QMA). The quasimacrospin approximation consists in modifying a micromagnetic calculation by additionally requiring that the system be uniformly magnetized. The free layer of the system is assumed to be a 3-nm-thick ellipse with major and minor semiaxis lengths of 32 and 16 nm, respectively. The material parameters correspond to permalloy (saturation magnetization $M_{\mathrm{s}} = 800$ G, exchange stiffness $A = 1.3 \times 10^{-6}$ erg cm^{-1}, anisotropy constant $K = 0$, and the Gilbert damping parameter $\alpha = 0.014$). The system used to model QMA was the same except for a factor of 16 larger exchange stiffness. For this system, the magnetization magnitude averaged over all cells differed from M_{s} by no more than 0.2% for all dynamic processes, being indicative of a highly spatially uniform magnetization. It was assumed that $a_J = 100$ Oe and $b_J = 0$ for $J = 10^7$ A cm^{-2}. To numerically integrate the GLLE (1), our program package SpinPM was utilized. In accordance with current practice, only calculations for the free layer were made [23]. The vector $\mathbf{m}_{\mathrm{ref}}$ was assumed to be along the x-axis, and the eddy field was assumed to contribute nothing.

The first case considered was structure switching by a current in a zero magnetic field. As it turned out, the QMA is quite adequate for describing both the structure switching current and the behavior of the layer- and time-averaged x-component of the magnetization (see Fig. 1). That measured switching currents agree well with the single-domain approximation has also been shown by other authors [7]. However, even for such a small structure the QMA-calculated switching time differed appreciably from (was about 10% larger than) the MMA result, which is in agreement with available experimental data [21].

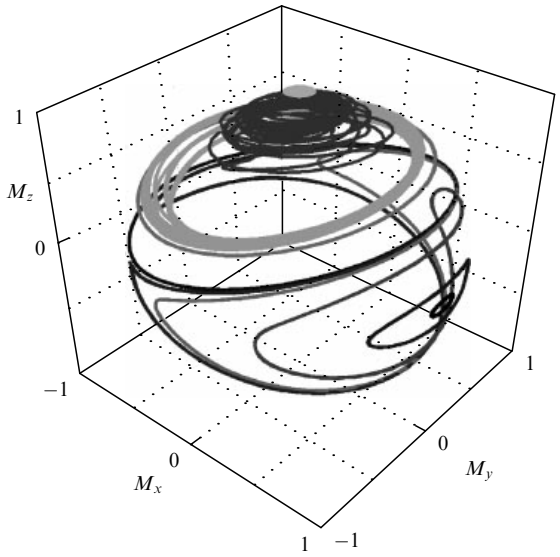

Figure 2. Mechanical trajectories of the layer-averaged and M_{s}-normalized magnetization vector of the free layer. MMP calculations are done for different values of the current (represented by different color hues) for a magnetic field $H = 1000$ Oe applied along the $-x$ direction.

The next case considered was one in which the application of an external magnetic field leads to the excitation of magnetization oscillations in the system. Figure 2 displays free-layer magnetization trajectories calculated in the MMA for an external magnetic field $H = 1000$ Oe. For sufficiently low currents, these trajectories are very nearly periodic in the sense that each curve passes within a close proximity of the point where it started. However, this periodicity is lost at a certain critical current density J_{ch}, the trajectories become to a large extent chaotic [24], and essentially nonuniform (multi-domain) states, occasionally containing vortices or distinct domain walls, start to develop in the system. Figure 3 depicts the Fourier spectra of the function $\langle M_x \rangle(t)$ for quasiperiodic (dark curve) and nonperiodic (light curve) trajectories. The first spectrum is a set of narrow peaks, among which one distinguishes the main peak and a set of its higher-order harmonic satellites. The second spectrum also exhibits the main peak, but it is very broad (with a width of more than 1 GHz).

Along with chaotization of system's magnetization trajectories, other effects are lost in QMA calculations. In Fig. 4 are shown MMA- and QMA-calculated positions of the main spectral peak f as functions of current density J. These dependences match almost exactly up to a certain critical value of J_{s} ($\approx 2.2 \times 10^7$ A cm^{-2} in Fig. 4) and start to noticeably differ above this value. It is important to note that in the general case $J_{\mathrm{s}} < J_{\mathrm{ch}}$ and that these dependences may differ sufficiently greatly — by several times. In the interval $J_{\mathrm{s}} < J < J_{\mathrm{ch}}$, spatially nonuniform spin wave modes are excited in the system [22] — one for every current density

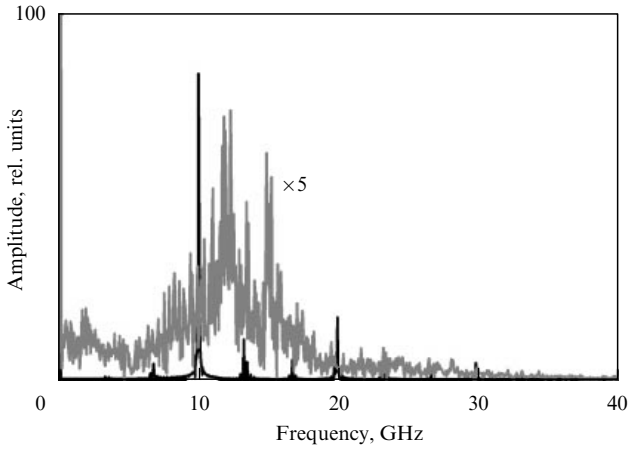

Figure 3. Fourier spectra of the layer-averaged x-component of magnetization $\langle M_x \rangle(t)$ of the free layer obtained for quasiperiodic ($j = 3 \times 10^7$ A cm^{-2}, $H = 10^3$ Oe) and nonperiodic ($j = 1 \times 10^8$ A cm^{-2}, $H = 10^3$ Oe) trajectories (dark and light curves, respectively).

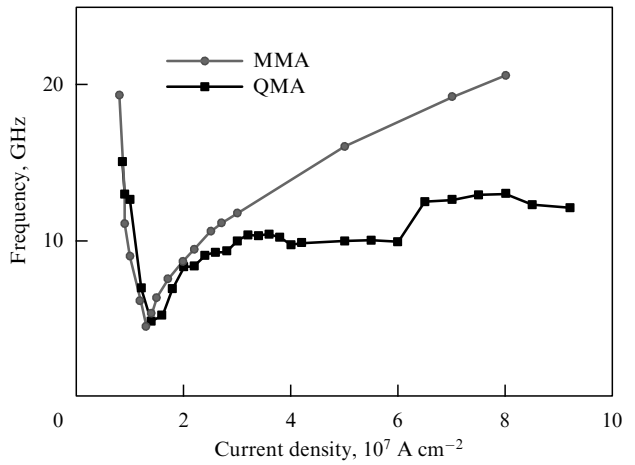

Figure 4. The position of the main frequency peak versus density current. Calculations are made in the MMA and QMA for an external magnetic field $H = 1000$ Oe.

value except for small J intervals where mode-to-mode transitions occur; the spectrum here is reduced to a narrow peak, and magnetization trajectories are quasiperiodic. For $J > J_{ch}$, several nonuniform spin wave modes are excited, which are comparable in amplitude and interact between themselves due to nonlinearities in the system — thus broadening the spectral peak and leading to chaotic mechanical trajectories.

Thus, even in the case of a very small free layer, treating a CPP system in the QMA means losing important information about its dynamics, in particular, the time of the full magnetization reversal in the switching regime; the frequency of the main spectral peak, and the onset of the regime when the magnetization trajectories become chaotic for the oscillations.

3. Current-induced motion of the domain wall in a nanowire of elliptic cross section

This section examines the solution of the GLLE (1) for a one-dimensional magnetic system comprising a DW, specifically for an infinitely long nanowire with an elliptic cross section. The system is allowed to have anisotropy of the easy-axis type with the easy axis directed along a structure's (z) axis. It is assumed that anisotropy of the easy-axis type can be present when the axis lies in the transverse plane (xy); for definiteness sake, the axis is specified to be along x. We denote the corresponding uniaxial anisotropy constants by K_u and K_p. The magnetization distribution is allowed to vary only along z-axis; the magnetostatic interaction is assumed to be taken into account by the coefficients K_u and K_p.

Using expressions (4) and (5) for the torques, the solution of the GLLE (1) for this system is approximately given by

$$\frac{\partial \varphi}{\partial z} = 0\,, \qquad \theta = 2 \arctan \exp\left[\frac{z - q(t)}{\Delta(\varphi)}\right], \tag{6}$$

where φ, θ are the polar angles, $q(t)$ determines the position of the DW's center, and $\Delta(\varphi) = [a/(K_u + K_p \sin^2 \varphi)]^{1/2}$ is the DW width. The functions $q(t)$, $\varphi(t)$ satisfy the system of equations

$$\dot{q} + c_J - \alpha \Delta \dot{\varphi} = \gamma \Delta \frac{K_p}{M_s} \sin 2\varphi\,, \qquad \alpha \dot{q} + d_J + \Delta \dot{\varphi} - \gamma \Delta H = 0\,. \tag{8}$$

For $K_p = 0$, $H = 0$, system (7) allows a solution of the form [25]

$$\dot{q} = -\frac{c_J + \alpha d_J}{\alpha^2 + 1}\,, \qquad \dot{\varphi} = \frac{1}{\alpha^2 + 1}\left(\frac{\alpha c_J - d_J}{\Delta}\right). \tag{8}$$

This solution describes the z-directed translational motion of the DW whose plane rotates with a constant angular velocity. It should be noted that both current-induced torques — the adiabatic and nonadiabatic — make their contributions to the stationary DW motion.

In most real systems, however, $K_p \neq 0$ (for example, due to the elliptic cross section of the nanowire). In this case, system (7) admits the solution $\dot{\varphi} = 0$ for $H = 0$:

$$\dot{q} = -\frac{d_J}{\alpha}\,, \qquad \sin 2\varphi = \frac{M_s}{\alpha \gamma \Delta K_p}(\alpha c_J - d_J)\,, \tag{9}$$

where the second of relationships (9) (with Δ being the DW parameter, and φ the DW plane angle) determines the existence range for the solution (cf. Ref. [26]). Solution (9) for constant current describes the constant-velocity DW motion with time-independent slope φ. Unlike the preceding case, here the adiabatic torque $\mathbf{T}_a$ has no effect on the steady velocity of the DW. The motion of the DW is determined only by the nonadiabatic torque $\mathbf{T}_{na}$. In the limiting case of a thin magnetic film, this solution was obtained in Refs [18, 19].

4. Current-induced motion of the domain wall in a CPP spin-valve structure

This section discusses the solution of the GLLE (1) for a multilayer DW-containing system with a current flowing

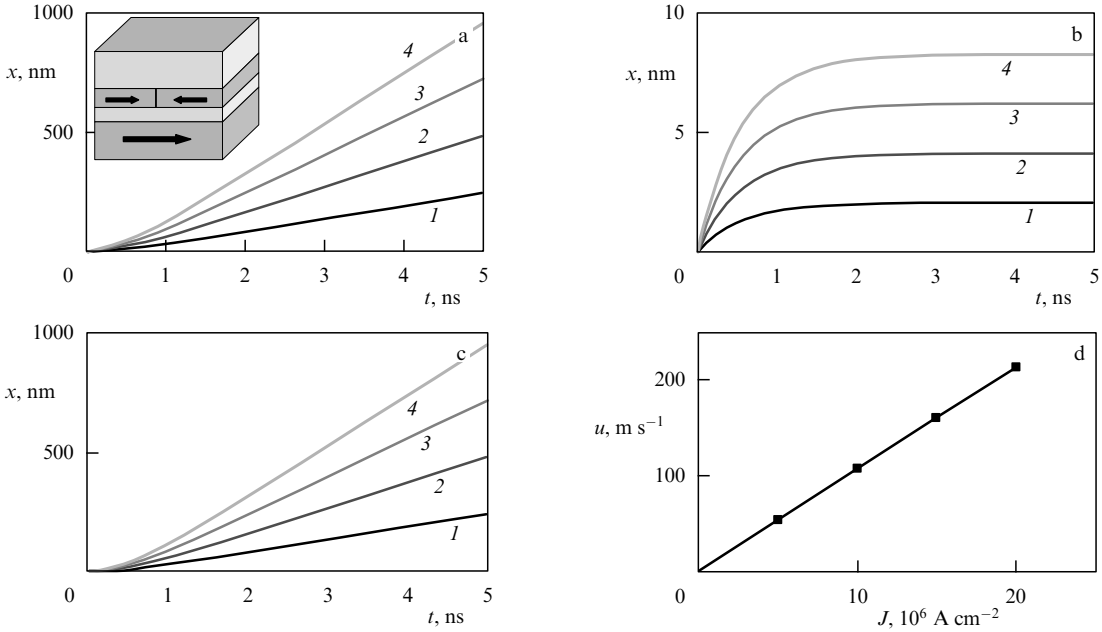

Figure 5. Current-induced DW displacements calculated for (a) the torques $\mathbf{T}_\parallel$ and $\mathbf{T}_\perp$ combined, (b) the torque $\mathbf{T}_\parallel$ alone, and (c) the torque $\mathbf{T}_\perp$ alone. Calculations are made for current densities $J = 5, 10, 15, 20$ [10^6 A cm^{-2}] (curves *1–4*, respectively). The upper limit for this set is $J = 24 \times 10^6$ A cm^{-2}, a current value at which the current-induced magnetization reversal of one of the domains occurs. The inset to panel (a) depicts the geometry of the system. (d) Velocity of stationary DW motion as a function of current density J.

perpendicular to the layers. As shown in the inset to Fig. 5a, the spin-valve structure under consideration consists, from the bottom up, of a layer with pinned magnetization (polarizer), a thin nonmagnetic spacer, a free magnetic layer, and a nonmagnetic metal contact. It is assumed that the free magnetic layer contains a single infinitely thin DW and that the layer with pinned magnetization is aligned in the positive z direction. There is a current flowing through this system, and the spin transfer effect can bring the DW into motion. A solution is sought for sufficiently low current densities for which each of the domains is, on its own, stable relative to current-induced excitation.

The solution method used was micromagnetic modeling, and the computations were limited to the free layer [23]. The influence of boundary effects was reduced by modeling the layer as a long strip (8 μm in length) 50×3 nm in cross section with a 'head-to-head' DW in its center. The magnetic parameters, chosen close to those of Co, were as follows: $M_s = 1400$ emu cm^{-3}, $A = 2 \times 10^{-6}$ erg cm^{-1}, and $\alpha = 0.007$. No bulk anisotropy was taken into account. The position of the DW at each instant of time was calculated from the system-averaged magnetization [27]. It was assumed that $a_J = 25$ Oe and $b_J = -2.5$ Oe for a current density $J = 10^7$ A cm^{-2}. To explore the role of the torques $\mathbf{T}_\parallel$ and $\mathbf{T}_\perp$ in DW motion, calculations for the same system were also carried out by considering these torques separately (which was rather a straightforward analysis due to the linearity of the system: the displacement of the DW under the action of the sum of $\mathbf{T}_\parallel$ and $\mathbf{T}_\perp$ is equal, to within 1% or less, to the sum of its displacements under the separate action of the torques $\mathbf{T}_\parallel$ and $\mathbf{T}_\perp$).

The results of the simulation are shown in Fig. 5. The domain wall starts moving at a finite velocity (Fig. 5a), accelerates for about 1 ns after switching on the current and then starts moving uniformly. As seen from Figs 5b and 5c, the initial velocity of the DW is determined by the action of the torque $\mathbf{T}_\parallel$, while its stationary motion depends exclusively on $\mathbf{T}_\perp$. When under $\mathbf{T}_\parallel$ (Fig. 5b), the DW starts moving at a finite velocity, but after a period of 1 ns it stops. Under $\mathbf{T}_\perp$ (Fig. 5c), the DW starts moving at zero velocity and then accelerates to a finite velocity. The velocity of the stationary DW motion is linear in the current (Fig. 5d).

There is a noteworthy similarity between this solution and that for CIP systems (see Refs [18, 19] and the results presented in Section 3) which consists, in particular, in a major torque not producing stationary DW motion. This similarity is due to the fact that the torques $\mathbf{T}_\parallel$ and $\mathbf{T}_\perp$ acting on a DW respectively in the CPP and CIP systems are — although different in origin — pointing in the same direction relative to the domain wall. The same is true for the pair of moments $\mathbf{T}_\perp$ and $\mathbf{T}_{na}$, either of which produces stationary DW motion [26].

Similar to what was done in Section 3, it is possible to construct a one-dimensional analytical model for this system [27]. According to this model, the velocity of the domain wall is given by the expression

$$u_{CPP} = -\frac{\gamma b_J \Delta}{\alpha} . \qquad (10)$$

This expression describes the simulation results to within about 10%. It is of interest to compare this result with that for DW motion in the CIP configuration [see formula (9)]. Taking $d_J = 0.007$ m s^{-1} at a current density $J = 10^6$ A cm^{-2} (the upper estimate for d_J according to Refs [18, 19]), it is found that $u = 1$ m s^{-1} for Co, whereas for our system ($\Delta = 19$ nm) Eqn (10) yields $u_{CPP} = 14$ m s^{-1} for the same value of J. A similar relation between u and u_{CPP} is observed in other 3d-metals and for typical geometries of the structure. Thus, in terms of current-induced DW excitation the spin-valve CPP structure can be an order of magnitude more efficient than the similar monolayer CIP structure, defining the efficiency as the DW velocity at a given current density.

This result, due to the fact that the torque $T_{\perp}$ is much larger than T_{na} in typical magnetic nanostructures, can be of practical importance for developing controlled magnetic elements (magnetic memory and logic) [28].

5. Spin current in molecular systems

One further class of experimental configurations for studying spin-current-induced effects comprises systems containing conducting organic molecules. Such molecules are grown by self-assembly methods and brought into contact with a nonmagnetic or ferromagnetic metal (for example, Au or Ni). Such a contact is created by the chemosorption of so-called thiol groups that form at that end of an organic molecule which is in contact with a metal electrode. An example of such organic molecules with thiol terminal groups is benzene-thiol molecules. To the other end of an organic molecule, a magnetic element (a magnetic nanocluster or an ion with the 'easy-plane' anisotropy) attaches itself, either chemically or by van der Waals forces. Another possible type of contact is the magnetic metallic (for example, Ni) probe tip of an atomic force microscope. Such an experimental configuration is currently typical in molecular spintronics.

At sufficiently low temperatures and low damping, the quantum effects show themselves in the dynamics of such a system [29]. A spin current induces excitations of a quasianion nature and gives rise to coherent quantum effects: Bloch oscillations in magnetic moment precession and tunneling effects between various quantum precession modes (so-called Zener macroscopic tunneling). These quantum effects can manifest themselves as jumps in the magnetic moment and peaks in the magnetic susceptibility of the system under consideration.

6. Conclusion

In this paper we have discussed various aspects of application of the Landau–Lifshitz equation modified by including additional, current-dependent torques. First, the study of the switching and oscillation dynamics of magnetization in CPP systems showed that the full-scale micromagnetic approach is of crucial importance even in the analysis of the smallest-sized systems. The analysis of CIP and CPP configurations of the systems with DWs showed that, although the current-induced spin torque $\mathbf{T}_{s.t.}$ is of a different origin in these two configurations, the solutions of the GLLE can be similar for certain system parameters. The reason for this lies in the fact that the corresponding components of the $\mathbf{T}_{s.t.}$ are pointing in the same direction relative to the domain wall. On the other hand, the current-induced DW motion in CPP structures can be more effective by far than in CIP structures. Finally, attention was brought to the quantum effects that spin-polarized current induces in molecular systems. The most noteworthy of these are Bloch-oscillating precession and Zener macroscopic tunneling of magnetization, both observed in sufficiently low-damping systems at low temperatures.

The work was supported by RFBR, project No. 07-02-91589.

References

1. Slonczewski J C *J. Magn. Magn. Mater.* **159** L1 (1996)
2. Berger L *Phys. Rev. B* **54** 9353 (1996)
3. Tsoi M et al. *Phys. Rev. Lett.* **80** 4281 (1998)
4. Myers E B et al. *Science* **285** 867 (1999)
5. Katine J A et al. *Phys. Rev. Lett.* **84** 3149 (2000)
6. Chappert C, Fert A, Nguyen Van Dau F *Nature Mater.* **6** 813 (2007)
7. Ralph D C, Buhrman R A, in *Concepts in Spin Electronics* (Ed. S Maekawa) (Oxford: Oxford Univ. Press, 2006) p. 195
8. Stiles M, Miltat J, in *Spin Dynamics in Confined Magnetic Structures III* (Eds B Hillebrands, A Thiaville) (Berlin: Springer-Verlag, 2006)
9. Vonsovskii S V *Magnetizm* (Magnetism) (Moscow: Nauka, 1971) [Translated into English (New York: J. Wiley, 1974)]
10. Brown W F (Jr.) *Micromagnetics* (New York: Wiley-Intersci., 1963)
11. Stiles M D, Zangwill A *Phys. Rev. B* **66** 014407 (2002)
12. Landau L, Lifshitz E *Phys. Z. Sowjetunion* **8** 153 (1935)
13. Barnaś J et al. *Phys. Rev. B* **72** 024426 (2005)
14. Edwards D M et al. *Phys. Rev. B* **71** 054407 (2005)
15. Zimmler M A et al. *Phys. Rev. B* **70** 184438 (2004)
16. Kiselev S I et al. *Nature* **425** 380 (2003)
17. Bazaliy Ya B, Jones B A, Zhang S-C *Phys. Rev. B* **57** R3213 (1998)
18. Li Z, Zhang S *Phys. Rev. B* **70** 024417 (2004)
19. Zhang S, Li Z *Phys. Rev. Lett.* **93** 127204 (2004)
20. Kimura T et al. *J. Appl. Phys.* **94** 7266 (2003)
21. Acremann Y et al. *Phys. Rev. Lett.* **96** 217202 (2006)
22. Krivorotov I N et al. *Phys. Rev. B* **76** 024418 (2007)
23. Miltat J et al. *J. Appl. Phys.* **89** 6982 (2001)
24. Berkov D V, Gorn N L *Phys. Rev. B* **72** 094401 (2005)
25. Khval'kovskii A V, Thesis for Candidate of Physicomathematical Sciences (Moscow: IOF RAN im. A.M. Prokhorova, 2006)
26. Tatara G, Kohno H *Phys. Rev. Lett.* **92** 086601 (2004)
27. Porter D G, Donahue M J *J. Appl. Phys.* **95** 6729 (2004)
28. Khval'kovskii A V et al. (in preparation)
29. Zvezdin A K, Zvezdin K A *Zh. Eksp. Teor. Fiz.* **122** 879 (2002) [*JETP* **95** 762 (2002)]